

First-order transition in the one-dimensional three-state Potts model with long-range interactions

Zvonko Glumac and Katarina Uzelac

Institute of Physics, POB 304, Bijenička 46, HR-10000 Zagreb, Croatia

The first-order phase transition in the three-state Potts model with long-range interactions decaying as $1/r^{1+\sigma}$ has been examined by numerical simulations using recently proposed Luijten-Blöte algorithm. By applying scaling arguments to the interface free energy, the Binder's fourth-order cumulant, and the specific heat maximum, the change in the character of the transition through variation of parameter σ was studied.

I. INTRODUCTION

The critical behavior of models with long-range (LR) interactions has been considerably less explored than that of the short-range (SR) ones, especially for discrete models where the non-locality of interactions makes most of the standard methods ineffective. These models may, however, exhibit rather complicated critical behavior already in one dimension [1–3,5]. Recent attention has been driven to such models in the context of studying phenomena related to LR interactions [6,7], but also in view of possible equivalence with SR models [6,8].

One of the interesting and still not clarified aspects of LR models is the possible onset of the first-order transition. The question naturally arises for the LR Potts model, which in the SR interaction case is known to undergo a first-order phase transition when the number of states q exceeds a certain limiting value which depends on dimensionality, $q_c(d)$ [9–11].

We have recently pointed out [12] that a similar behavior indeed can be observed in the $1d$ Potts model with interactions decaying with distance as $1/r^{1+\sigma}$ and illustrated it on special cases $q = 5, \sigma = 0.2$ and $q = 3, \sigma = 0.8$ characteristic of the two regimes. On the basis of these preliminary Monte Carlo (MC) results on small chains for $q = 3$ and $q = 5$, we have concluded on the existence of a q -dependent threshold value $\sigma_c(q)$ separating the first- and the second-order transition regime.

In the present paper, we focus on a more detailed study of the $1d$ three-state Potts model with $0 < \sigma < 1$.

As is well known, the first-order phase transitions are rather difficult to detect and study [13]. Most of standard renormalization group (RG) approaches do not distinguish them from the second-order transitions.

On the other hand Monte Carlo simulations, which in combination with finite-size scaling (FSS) represent an

efficient tool [14] to solve this problem, are limited when the first-order transition is weak, so that the correlation length, although finite, exceeds the considered system size. This problem is even more pronounced when dealing with LR interactions, where MC simulations become much more time consuming, no matter whether Metropolis or different cluster algorithms are used.

Recently, Luijten and Blöte [15] have proposed a rather efficient algorithm which permits considering quite large sizes in spite of the long-range interactions. Our intention is to use this approach here in order to perform a more systematic analysis of several quantities (interface free energy, Binder's fourth order cumulant, specific heat), which serve as criteria for distinguishing first- from second-order phase transition.

II. MODEL AND METHOD

The model we consider is defined by the Hamiltonian

$$H = - \sum_{i < j} \frac{J}{|i - j|^{1+\sigma}} \delta(s_i, s_j), \quad (1)$$

where $J > 0$, s_i and s_j denote three-state Potts variables at sites i and j , respectively, δ is the Kronecker symbol and summation is taken over all pairs of the system.

This model has a phase transition at finite temperature for $0 < \sigma \leq 1$ [3–5]. No exact results exist for the related critical behavior. By analogy with the SR interaction case extended to arbitrary dimension, one expects to find a first-order phase transition for low values of σ and a crossover to a second-order phase transition above a certain threshold value σ_c . This has been confirmed by our preliminary MC results [12] in $1d$ LR Potts model which lead to the conclusion, that for $q > 2$ the transition is of the first-order when $\sigma < \sigma_c(q)$ and of second order above it. The threshold $\sigma_c(q)$ is expected to depend on q . For $q = 3$, the σ_c was estimated [12] to lay above $\sigma_{MF} = 0.5$, the point separating the mean-field (MF) from the non-trivial critical regime in the Ising ($q = 2$) case (where the transition, by symmetry reasons (see e.g. ref. [9] and references therein), remains of the second order [16] in both regimes). Above the threshold σ_c , the model undergoes a second-order transition with non-classical critical exponents depending on σ . Several renormalization group approaches yield approximate values of these exponents, within continuous Ginzburg-Landau functional formalism [17] or in real space [3,5,7]. These latter approaches,

however, appear to be insensitive to detect a first-order transition.

In the present approach we shall be using the MC algorithm, recently introduced by Luijten and Blöte [15], designed for models with LR interactions. It is based on Wolf's cluster algorithm [18] and was applied to several MF related problems in the special (Ising) case $q = 2$ [8,19].

The basic idea of the method is the use of cumulative bond probabilities in building the cluster of connected bonds, which drastically reduces the number of operations required. The results coincide with those obtained with the simple Wolf algorithm, but the CPU time can be reduced by several orders of magnitude.

The basic quantity in our calculations is the energy probability distribution defined by

$$P_L(E) = \frac{1}{Z_L(K)} \mathcal{N}_L(E) e^{-KE}, \quad (2)$$

where $K = 1/T$ is the inverse temperature, $J = k_B$, Z is the partition function, $\mathcal{N}_L(E)$ denotes the number of spin configurations corresponding to the energy E , and L is the system size.

Several quantities used for the determination of the temperature driven first-order transition can be deduced from $P_L(E)$. We concentrate here on three most important ones: the interface free energy, the Binder's fourth order cumulant [20], and specific heat.

The interface free energy is obtained from the shape of the energy probability distribution $P_L(E)$. For temperature driven first-order transitions, at the transition temperature, $P_L(E)$ has two maxima, corresponding to the coexisting ordered and disordered phases. The interface free energy is then defined by

$$\Delta F_L = \ln \left. \frac{P_{LMax}}{P_{Lmin}} \right|_{K_L}, \quad (3)$$

where the finite-chain transition temperature K_L^{-1} has been defined by requiring that the two maxima are of equal height P_{LMax} . P_{Lmin} denotes the minimum of $P_L(E)$ between them.

The scaling analysis of ΔF_L can be used to identify the first-order phase transition, even in the case of a weak first-order transition, where the correlation length, though finite, is large and comparable to the system size [21]. When the transition is of the first-order, ΔF_L increases with size. For systems with SR interactions the interface free energy has the dimension of surface and scales as $\Delta F_L \sim L^{d-1}$. In the present model with LR interactions it is expected to scale as a volume.

The other two quantities can be derived from the higher energy momenta of $P_L(E)$, defined as

$$\langle E^n \rangle_L = \sum_E E^n P_L(E). \quad (4)$$

The specific heat C_L (defined per spin in the remaining text) is related to the second moment and defined for the system size L by

$$C_L = \frac{K^2}{L^d} (\langle E^2 \rangle_L - \langle E \rangle_L^2) . \quad (5)$$

According to the FSS theory, in the case of a second-order phase transition its maximum scales as

$$C_{LMax} \sim L^{\alpha/\nu}, \quad (6)$$

while for the first-order one it simply scales as volume which in the present case means linear dependence on L

$$C_{LMax} \sim L. \quad (7)$$

The calculation of the fourth moment gives Binder's fourth order cumulant [20] defined as

$$V_L^{(4)} = 1 - U_L^{(4)}/3, \quad (8)$$

where

$$U_L^{(4)} = \frac{\langle E^4 \rangle_L}{\langle E^2 \rangle_L^2}. \quad (9)$$

In the present study, for practical reasons it is easier to deal with $U_L^{(4)}$. In the thermodynamic limit $U_L^{(4)}$ tends to one, when $K \neq K_c$. At $K = K_c$ it still tends to one if the transition is of the second order, while it tends to a different constant in the case of a first-order transition. Together with ΔF , $U^{(4)}$ appears as one of the most sensitive criteria for determination of first-order phase transitions [20,22].

A. The special case $\sigma = -1$

Before proceeding to the presentation of our numerical results, let us summarize the only analytical results available for the considered model. They can be obtained in the limit $\sigma = -1$ of model (1), where all the interactions are of equal strength and the coupling constant is redefined so that $K \rightarrow K/L$. This is the mean-field limit, which has been extensively studied in literature (see e.g. [9]) and solved in the limit $L \rightarrow \infty$ by saddle point method [23].

The energy E and the entropy S of this model to the leading order in L writes

$$\frac{E}{L} = -\frac{1}{2} \sum_{m=0}^{q-1} \left(\frac{L_m}{L} \right)^2, \quad (10)$$

$$\frac{S}{L} = -\sum_{m=0}^{q-1} \frac{L_m}{L} \ln \left(\frac{L_m}{L} \right), \quad (11)$$

where L_m 's, the numbers of particles in the m -th Potts state, satisfy the condition $L_0 + \dots + L_{q-1} = L$. The transition temperature, the order parameter jump and the latent heat are known [23] for the above model.

To the best of our knowledge, the results for the characteristic quantities $U_{Max}^{(4)}$ and C_{Max} were not cited in literature. In order to obtain them, we have used the Lee and Kosterlitz [22] prescription for the energy probability distribution $P_L(E)$ in the vicinity of the first-order transition temperature K_c^{-1} for large L ,

$$P_L(E) = \frac{f(Lt) \delta(E - E_o) + \delta(E - E_{do})}{f(Lt) + 1}, \quad (12)$$

where $t = (K - K_c)/K_c$, and E_o and E_{do} are the energies of ordered and disordered phases, respectively. The weight function $f(Lt)$ which contains the entire temperature and L dependence of $P_L(E)$ is not given explicitly. Only the limiting behavior of $f(Lt)$, $f(x \rightarrow -\infty) \rightarrow 0$ and $f(x \rightarrow \infty) \rightarrow +\infty$, is required, in order to have only one δ -function in thermodynamic limit for temperatures above or below the transition temperature, while for finite L the two δ -functions coexist. Maximizing $U_L^{(4)}$ and C_L with respect to temperature fixes the value of the function $f(Lt)$ and leads to

$$\lim_{L \rightarrow \infty} U_{LMax}^{(4)} = \left[1 + \frac{(q-2)^4}{2(q-1)(q^2-3q+3)} \right]^2 \quad (13)$$

and

$$\lim_{L \rightarrow \infty} \frac{C_{LMax}}{L} = \left[\frac{q-2}{2q} \ln(q-1) \right]^2. \quad (14)$$

For finite L , the exact calculations may be performed numerically for very large sizes ($L = 100\,000$ is easily attained). They match well with the analytical results (13) and (14) and justify the conjecture (12) from which they were derived.

III. NUMERICAL RESULTS

By using the Luijten-Blöte cluster algorithm, we have been able to reach sizes up to 5 000 with reasonable computing time. The systematic simulations were performed for sizes L ranging from 200 to 3 000, with periodic boundary conditions. The parameter σ was taken with the increment of 0.1 in the interval $0 < \sigma < 1$, where the nontrivial transition is to be expected. For each set of parameters, 10^6 clusters were generated. Let us also point out that the characteristic temperatures related to the three quantities considered are different until the thermodynamic limit is reached. Consequently, an independent numerical effort was needed for localizing the characteristic temperatures for each of those

quantities for every L and σ considered. By combining the Ferrenberg-Swendsen histogram method [24] and direct calculations, these temperatures have been calculated with numerical precision up to the fourth decimal digit in K_L , which implies a numerical error of approximately 0.1%. We did not go beyond this precision in K_L since the aspect of the calculated distribution $P_L(E)$ is much rougher than the one obtained with the Metropolis algorithm, when using a comparable number of steps. Resulting numerical error in calculated quantities themselves varies from 1-5 % for $P_L(E)$ and ΔF_L to 1-2% for C_{LMax} and $U_{LMax}^{(4)}$.

A. Interface free energy

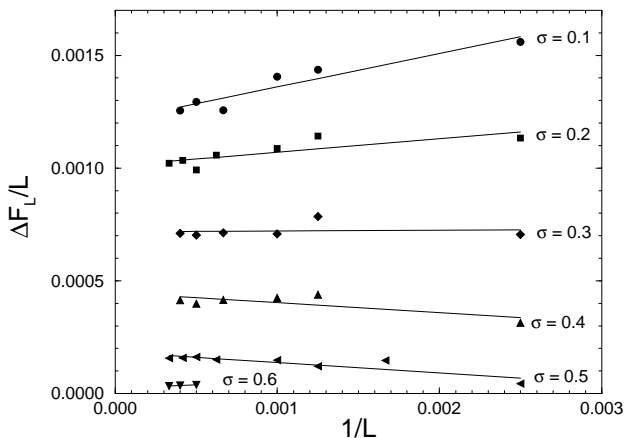


FIG. 1. Interface free energy divided by size versus inverse size. Data for $\sigma = 0.1$ to 0.6 are included. Lines are obtained by linear regression.

In Fig. 1 are presented the results for the interface free energy divided by size versus $1/L$. Only sizes $L \geq 400$ are included. Points of different shapes correspond to data with different σ . It ranges from 0.1 to 0.6, where, within considered sizes, the two maxima of $P_L(E)$ could be discerned beyond the error limits. For $\sigma = 0.6$ this occurs only when $L \geq 2\,000$.

The lines represent the fit of $\Delta F_L/L$ to linear form and illustrate the leading correction to the expected scaling form $\Delta F \sim L$, and show good agreement with it.

The weakening of the transition is manifested by the fact that $\Delta F_L/L$ becomes smaller with increasing σ . This dependence is almost linear unless σ gets close to the assumed onset of the second order regime.

The other two quantities, $U_L^{(4)}$ and C_{LMax} , derived from momenta (Eqs. (5) and (9)), have been calculated in the entire region $0 < \sigma < 1$.

B. Binder's fourth order cumulant

In order to find out whether in the thermodynamic limit $U_{LMax}^{(4)}$ will tend to one or to a different value, we analyze the maxima of $U_L^{(4)}(K)$ as functions of L . The

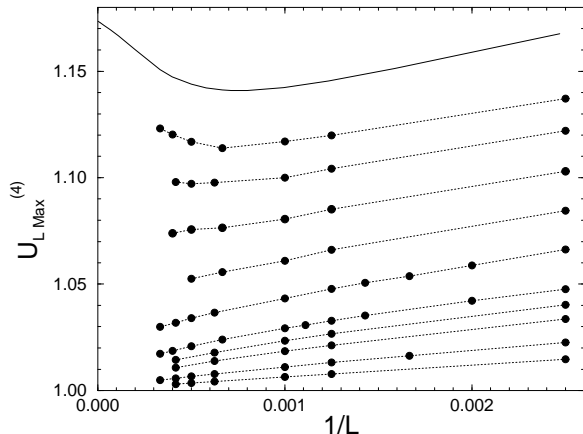


FIG. 2. Fourth-order cumulant as a function of inverse size. Points connected with dotted lines correspond to $\sigma = 0.1, 0.2, 0.3, 0.4, 0.5, 0.6, 0.65, 0.7, 0.8, 0.9$, from top to bottom. The solid line denotes the results for $\sigma = -1$ limit.

results for $U_{LMax}^{(4)}$ are summarized in Fig. 2, where the $\sigma = -1$ results are also traced for comparison. For low values of σ , $U_{LMax}^{(4)}$ is non-monotonic in $1/L$, similar to the $\sigma = -1$ case, so that in the $L \rightarrow \infty$ limit it is clearly different from unity. For higher values of σ , where the

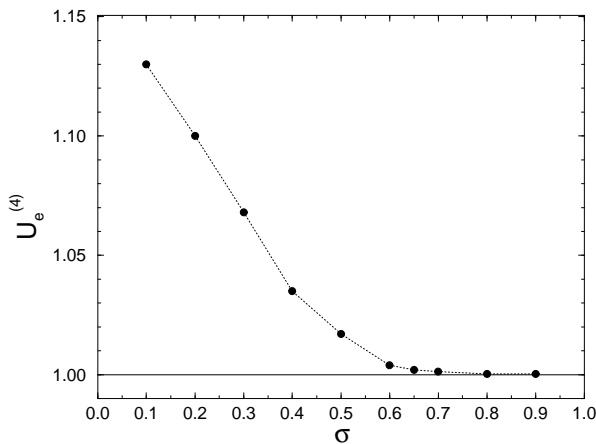


FIG. 3. Extrapolated values of the fourth-order cumulant as a function of σ . The constant line at unity is drawn to guide the eye.

behavior is monotonous, the fit to the power-law form $U_{LMax}^{(4)} = U_e^{(4)} + const. \cdot L^x$ was made. The extrapolated results for $U_e^{(4)}$ are presented on Fig. 3. One can observe that the transition between the two regimes occurs in a continuous and smooth way with the change of σ . For $\sigma \leq 0.6$ we obtain $U_e^{(4)} \neq 1$ outside the estimated error bars (given by the size of the points). Also, for $\sigma \geq 0.7$ we conclude that, within the error bars, $U_e^{(4)}$ has reached unity. The additional point 0.65 can be attributed to both regimes.

These results are consistent with the above ones for ΔF .

C. Specific heat

The data for the specific heat maxima C_{LMax} are summarized in Fig. 4 in the form of C_{LMax}/L versus $1/L$. According to Eqs. (6) and (7) and by taking into ac-

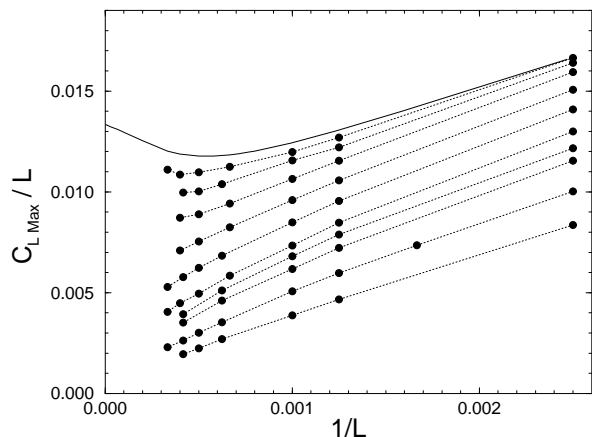


FIG. 4. Maxima of the specific heat divided by size versus inverse size. Solid line denotes the case $\sigma = -1$. Points connected with dotted lines correspond to $\sigma = 0.1, 0.2, 0.3, 0.4, 0.5, 0.6, 0.65, 0.7, 0.8, 0.9$, from top to bottom.

count that α/ν is much smaller than unity in the region of interest, C_{LMax}/L should tend to a constant or to zero value, depending on whether the transition is of the first- or second-order, respectively.

Similar as for $U_L^{(4)}$, the curves are non-monotonic and tend to a nonzero value in the $\sigma = -1$ case and for low values of σ . For higher values of σ the convergence to limit $L \rightarrow \infty$ was examined by the fit to the form $C_{LMax}/L = c_0 + const. \cdot L^{-x}$. The constant c_0 is nonzero in the first-order regime, while in the second-order one $c_0 = 0$ and $x = 1 - \alpha/\nu$. This means also that the log-log plot of the curves of Fig. 4 should have a linear

shape in the latter case, while it will deviate from the straight line in the former case. In Fig. 5 log-log plots of C_{LMax}/L versus $1/L$ are given for $\sigma \geq 0.5$. The curves for 0.5 and 0.6 clearly leave the straight line. Linear

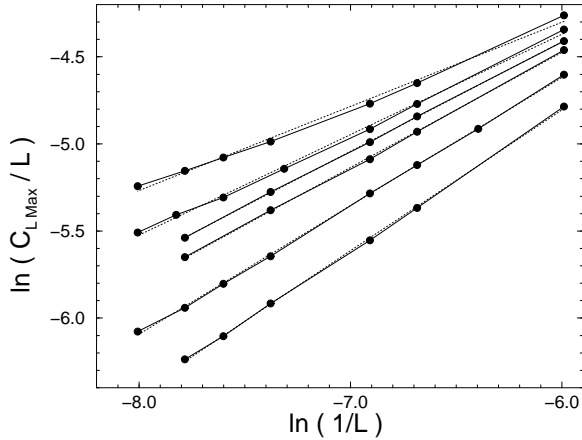


FIG. 5. Log-log plot of the maxima of the specific heat versus inverse size. The points connected by solid lines represent the results for $\sigma = 0.5, 0.6, 0.65, 0.7, 0.8$ and 0.9 , from top to bottom. Dotted lines denote the fit to the straight line by linear regression.

fit is very good for $\sigma \geq 0.65$, indicating the second-order transition. The corresponding critical exponent α/ν following from the fit for $\sigma = 0.65, 0.7, 0.8, 0.9$ is $0.36, 0.33, 0.26, 0.19$, respectively, which is in poor agreement with values expected from the finite-range scaling (FRS) [5] calculations, which for the same values of σ would give $\alpha/\nu = 0.32, 0.27, 0.15, -0.02$. One should mention, however, that it is generally a difficult task to extract critical exponents with good precision from the specific heat maxima [26].

D. Critical temperature

The three different characteristic temperatures arise in calculation of ΔF_L and maxima of $U_L^{(4)}(K)$ and $C_L(K)$, which all should tend to the critical temperature in the thermodynamic limit. The $L \rightarrow \infty$ extrapolations of these quantities made by assuming power-law corrections in $(1/L)$ are presented in Table I, compared to the existing earlier results obtained by FRS [5] and RG [7]. The extrapolation errors are estimated to be in the limits (± 0.01) which is also comparable to difference between the extrapolations obtained from different characteristic temperatures. The agreement with the FRS results is quite good, discrepancy does not exceed 5 %, except for $\sigma = 0.1$, where the convergence of FRS is weakest, and the extrapolation errors in both methods are largest.

(For $\sigma = 0.1$ all the calculations were thus performed up to the sizes $L = 5000$.) The RG results appear to be systematically larger than ours, and the discrepancy with them varies from 7 to 33 %. Similar discrepancy is obtained for the fit to the functional form $K_c \sim \sigma$ in the limit $\sigma \rightarrow 0$, conjectured in ref. [6].

TABLE I. Inverse critical temperatures ($K_e(C)$, $K_e(U^{(4)})$, $K_e(\Delta F)$), obtained by extrapolation of K_L compared to FRS extrapolated values ($K(FRS)$) [5] and RG results ($K(CM)$) [7].

σ	$K_e(C)$	$K_e(U^{(4)})$	$K_e(\Delta F)$	$K(FRS)$	$K_e(CM)$
0.1	0.16	0.15	0.16	0.14	0.15
0.2	0.28	0.28	0.27	0.270	
0.3	0.38	0.38	0.37	0.386	0.43
0.4	0.49	0.49	0.48	0.494	
0.5	0.58	0.60	0.59	0.601	0.71
0.6	0.71	0.71	0.71	0.714	
0.65	0.78	0.77		0.774	
0.7	0.84	0.84		0.837	1.05
0.8	0.98	0.99		0.977	
0.9	1.14	1.13		1.144	1.64

IV. CONCLUSION

We have applied MC simulations in combination with FSS in order to examine the onset of the first-order phase transition in the $1d$ three-state Potts model with long-range interactions. The Luijten-Blöte advanced algorithm for long-range interaction systems allowed us to treat successfully considerably large sizes (up to 3000) in a reasonable amount of time, in spite of the long range of interactions. The systematic analysis of three quantities: the interface free energy, Binder's fourth order cumulant, and specific heat, confirms the existence of two regimes in the interval $0 < \sigma \leq 1$. All three considered quantities give the first-order transition for $\sigma \leq 0.6$. The transition becomes gradually weaker with increasing σ and changes smoothly to a second-order transition by continuous variation of σ .

For the sizes examined here (up to 3000) and within the estimated error bars, we obtain a second-order transition for $\sigma \geq 0.7$.

The present approach has, however, limitations to precise determination of the threshold. Since the transition close to the threshold becomes arbitrarily weak, the finite correlation length, characteristic of the first-order transition, will always be much larger than the size of the

considered system, close enough to σ_c . Thus, the present result for σ_c should be understood only as a lower limit for the possible onset of the second-order phase transition.

For this purpose rather complementary studies should be done, such as the one on the dependence of the finite correlation length on σ .

It is interesting to notice at the end that, according to present results, $\sigma_c(q = 3)$ falls in the interval between 0.6 and 0.7. If the correspondence between SR and LR models [8] would be extended outside the MF regime to the present problem and to the Potts model, it would lead to the conjecture $\sigma_c(q = 3) = 2/d_c(q = 3)_{SR}$ which would give $\sigma_c(q = 3)$ close to and slightly larger than 0.66. However, this line of argument would also imply that $\sigma_c = 1$ already for $q = 4$.

- [22] J. Lee J and J. M. Kosterlitz, Phys. Rev. B **43**, 3265 (1991).
- [23] T. Kihara, Y. Midzuno and T. Shizume, J. Phys. Soc. Jpn. **9**, 681 (1954).
- [24] A. M. Ferrenberg and R. H. Swendsen, Phys. Rev. Lett. **61**, 2635 (1988).
- [25] see e. g. H. W. J. Blöte and R. H. Swendsen, Phys. Rev. Lett. **43**, 799 (1979) and references in [9].
- [26] C. Holm and W. Janke, Phys. Rev. B **48**, 936 (1993); C. Holm and W. Janke, J. Phys. A **27**, 2553 (1994).

-
- [1] F. J. Dyson, Commun. Math. Phys. **12**, 91 (1969).
 - [2] J. M. Kosterlitz, Phys. Rev. Lett. **37**, 1577 (1976).
 - [3] J. L. Cardy, J. Phys. A **14**, 1407 (1981).
 - [4] M. Aizenman, J.T. Chayes, L. Chayes, C.M. Newman, J. Stat. Phys. **50**, 1, 1988)
 - [5] Z. Glumac and K. Uzelac, J. Phys. A **26**, 5267 (1993).
 - [6] C Tsallis, Fractals **5**, 541 (1995).
 - [7] S. A. Cannas and A. C. N. de Magalhães, J. Phys. A **30**, 3345 (1997).
 - [8] E. Luijten and H. W. J. Blöte, Phys. Rev. Lett. **76**, 1557 (1996).
 - [9] F. Y. Wu, Rev. Mod. Phys. **54**, 235 (1982).
 - [10] R. J. Baxter, J. Phys. C: Solid State Phys. **6**, L445 (1973).
 - [11] A. Aharony and E. Pytte, Phys. Rev. B **23**, 362 (1981).
 - [12] K. Uzelac and Z. Glumac, Fizika B **6**, 133 (1997).
 - [13] W. Janke and R. Villanova, Nucl. Phys. B **489** [FS], 679 (1997); W. Janke, in *Computer Simulations in Condensed Matter Physics VII*, eds. D. P. Landau, K. K. Mon and H. B. Schüttler (Springer-Verlag, Berlin, 1994).
 - [14] K. Binder and H. J. Herrmann, in *Monte Carlo Simulation in Statistical Physics*, eds. M. Cardona, P. Fulde, K. von Klitzing and H.-J. Queisser (Springer-Verlag, Berlin, 1992).
 - [15] E. Luijten and H. W. J. Blöte, Int. J. Mod. Phys. C **6**, 359 (1995).
 - [16] M. Aizenman, R. Fernández, Lett. Math. Phys. **16**, 39 (1988)
 - [17] R. G. Priest and T. C. Lubensky, Phys. Rev. B **13**, 4159 (1976); W. K. Theumann and M. A. Gusmão, Phys. Rev. B **31**, 379 (1985).
 - [18] U. Wolf, Phys. Rev. Lett. **62**, 361 (1989).
 - [19] E. Luijten and H. W. J. Blöte, Phys. Rev. B **56**, 8945 (1997).
 - [20] K. Binder, Phys. Rev. Lett. **47**, 693 (1981).
 - [21] J. Lee J and J. M. Kosterlitz, Phys. Rev. Lett. **65**, 137 (1990).